Theoretical and Experimental Study of Charge Transfer Through DNA: Impact of Mercury Mediated T-Hg-T Base Pair.

ARTICLE *in* THE JOURNAL OF PHYSICAL CHEMISTRY B · APRIL 2014

Impact Factor: 3.3 · DOI: 10.1021/jp501986a · Source: PubMed

11 AUTHORS, INCLUDING:

Martin Vala
Brno University of Technology
59 PUBLICATIONS **243** CITATIONS
SEE PROFILE

Martin Weiter
Brno University of Technology
73 PUBLICATIONS **309** CITATIONS
SEE PROFILE

Yoshiyuki Tanaka
Tokushima Bunri University
80 PUBLICATIONS **2,013** CITATIONS
SEE PROFILE

F. Matthias Bickelhaupt
VU University Amsterdam
376 PUBLICATIONS **11,444** CITATIONS
SEE PROFILE

THE JOURNAL OF PHYSICAL CHEMISTRY B

Article

pubs.acs.org/JPCB

Theoretical and Experimental Study of Charge Transfer through DNA: Impact of Mercury Mediated T-Hg-T Base Pair

Irena Kratochvílová,*[,†,‡] Martin Golan,[†,§] Martin Vala,[∥] Miroslava Špérová,[∥] Martin Weiter,[∥] Ondřej Páv,*[,⊥] Jakub Šebera,[†,⊥] Ivan Rosenberg,[⊥] Vladimír Sychrovský,[⊥] Yoshiyuki Tanaka,[#] and F. Matthias Bickelhaupt[▽,○]

[†]Institute of Physics, Academy of Sciences of the Czech Republic, v.v.i, Na Slovance 2, CZ-182 21 Prague 8, Czech Republic

[‡]Faculty of Nuclear Physics and Physical Engineering, Czech Technical University in Prague, Zikova 1, 160 00 Prague 6, Czech Republic

[§]Institute of Physics, Faculty of Mathematics and Physics, Charles University in Prague, Ke Karlovu 5, CZ-121 16 Prague 2, Czech Republic

[∥]Materials Research Centre, Faculty of Chemistry, Brno University of Technology, Purkyňova 118, CZ-612 00 Brno, Czech Republic

[⊥]Institute of Organic Chemistry and Biochemistry, Academy of Sciences of the Czech Republic, v.v.i., Flemingovo náměstí 2, CZ-16610 Prague 6, Czech Republic

[#]Graduate School of Pharmaceutical Sciences, Tohoku University, 6-3 Aza-Aoba, Aramaki, Aoba-ku, Sendai, Miyagi 980-8578, Japan

[▽]Department of Theoretical Chemistry and Amsterdam Center for Multiscale Modeling (ACMM), VU University Amsterdam, De Boelelaan 1083, 1081 HV Amsterdam, The Netherlands

[○]Institute for Molecules and Materials (IMM), Radboud University Nijmegen, Comeniuslaan 4, 6525 HP Nijmegen, The Netherlands

Supporting Information

ABSTRACT: DNA-Hg complexes may play an important role in sensing DNA defects or in detecting the presence of Hg in the environment. A fundamental way of characterizing DNA-Hg complexes is to study the way the electric charge is transferred through the molecular chain. The main goal of this contribution was to investigate the impact of a mercury metal cation that links two thymine bases in a DNA T-T mismatched base pair (T-Hg-T) on charge transfer through the DNA molecule. We compared the charge transfer efficiencies in standard DNA, DNA with mismatched T-T base pairs, and DNA with a T-Hg(II)-T base pair. For this purpose, we measured the temperature dependence of steady-state fluorescence and UV−vis of the DNA molecules. The experimental results were confronted with the results obtained employing theoretical DFT methods. Generally, the efficiency of charge transfer was driven by mercury changing the spatial overlap of bases.

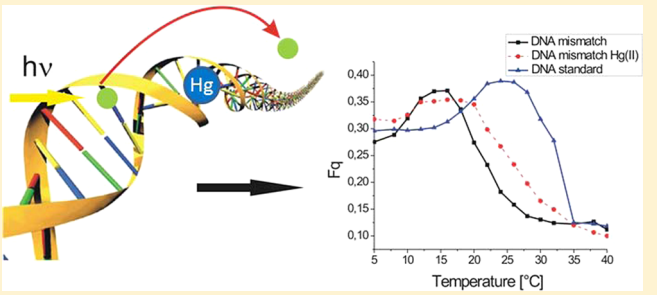

1. INTRODUCTION

As the carrier of genetic information, deoxyribonucleic acid (DNA) holds an extremely important position in the field of biology, biochemistry, and biophysics.[1−19] In particular, the ability of oligonucleotides to mediate charge transfer provides the basis for novel molecular devices and plays a role in the processes of sensing and/or repair of molecular damage.[1,2] Several studies have been reporting that a guanine triplet sequence tends to undergo one electron oxidation reaction and the developed charge can move through the adenine−thymine base pair (A−T).[9,11] This charge transport mechanism has been discussed in relation with DNA damage and repair.[14]

One of the most promising approaches to modifying DNA properties is to form metal−DNA complex systems. For example, platinum(II) complexes such as cisplatin, which is known as an antitumor drug, distort the structure of the DNA duplex by coordinating Pt to the N7 atom of guanine located in the outer region of the duplex.[3] Recently, Ono et al.[20−25] have demonstrated that a thymine−thymine mismatch base pair (T−T) in a DNA duplex captured the Hg(II) ion to form a stable neutral thymine−mercury(II)−thymine base pair (T-Hg(II)-T). DNA/Hg complexes play an important role in probing defects in DNA or the presence of Hg in the environment. An important way of characterizing DNA/Hg complexes is investigating the way electric charge is transferred through them.

Received: February 25, 2014
Revised: April 26, 2014

   dx.doi.org/10.1021/jp501986a | J. Phys. Chem. B XXXX, XXX, XXX−XXX

Table 1. DNA Duplexes for UV−Vis and Fluorescence Spectroscopy Measurements[a]

Sample Description	Sequence
DNA standard redox active	5′-d(TIA ITAp AAG TTA IA)-3′ 3′-d(ACT CAT TTC AAT CT)-5′
DNA standard redox inactive	5′-d(TIA ITAp AAI TTA IA)-3′ 3′-d(ACT CAT TTC AAT CT)-5′
DNA mismatch redox active	5′-d(TIA ITAp TAG TTA IA)-3′ 3′-d(ACT CAT TTC AAT CT)-5′
DNA mismatch redox inactive	5′-d(TIA ITAp TAI TTA IA)-3′ 3′-d(ACT CAT TTC AAT CT)-5′
DNA mismatch Hg(II) redox active o: -Hg(II)-	5′-d(TIA ITAp TAG TTA IA)-3′ ○ 3′-d(ACT CAT TTC AAT CT)-5′
DNA mismatch Hg(II) redox inactive o: -Hg(II)-	5′-d(TIA ITAp TAI TTA IA)-3′ ○ 3′-d(ACT CAT TTC AAT CT)-5′

[a]In the redox-active duplexes, the hole acceptor was guanine (G), and the hole donor was 2-aminopurine (Ap). In the redox-inactive duplexes, G was replaced by redox-inactive inosine (I). Other symbols indicate standard nucleobases in the oligonucleotide sequences. DNA T-T mismatch molecules were bridged by Hg(II) in the case of DNA mismatch Hg(II) redox active and DNA mismatch Hg(II) redox inactive duplexes.

In this work, we studied the DNA-Hg complex's properties and behavior from the point of view of a specific physical parameter: charge transfer. Thymine−Hg(II)−thymine complexes could play an important role in the design of devices for possible application in DNA-based biosensors.[26−31]

T-Hg(II)-T complexes have very interesting properties: the thermally induced transition profile of a duplex containing the T−T mismatch is shifted to higher temperature in the presence of Hg(II) ions.[25] The T−Hg(II)−T structure is even more stable than the Watson−Crick (WC) A−T.[25] Despite a lot of effort being devoted to the investigation of metal−oligonucleotide complexes, there are many fundamental issues that have not been explained.

Here, we extended our previous studies[6−8] on charge transfer in oligonucleotides with various base-pairing patterns and investigated the impact of mercury bonded to mismatched DNA bases on the charge transfer process. We compared the charge transfer efficiencies of standard DNA, DNA with mismatched (T-T) base pair (DNA T-T), and DNA with T−Hg(II)−T (DNA T−Hg(II)−T). For this purpose, we measured the temperature dependence of steady-state fluorescence and UV−vis spectroscopy. Our experimental results were confronted with theoretical results obtained using the density functional theory (DFT). We measured how the short distance charge transfer efficiency was affected by specific DNA-Hg(II) complex properties. Our results revealed the detailed interplay between the efficiency of charge transfer and basic physicochemical properties of oligonucleotides, providing a significant contribution not only to biochemistry but also to the potential future utilization of these materials in nanotechnology.

2. MATERIALS AND METHODS

2.1. Sample Preparation and Characterization. Three general types of duplexes were prepared (Table 1): DNA composed of two DNA strands, where the donor−acceptor pairs 2-aminopurine (Ap)−guanine (G) were separated by two bases with standard (Figure S1, Supporting Information) and mismatched base pair setting close to Ap. The duplexes containing the Ap and G are called redox active. In all measurements, Ap represented an optically excited fluorescent redox probe introduced into the DNA chain as a hole donor. The charge developed upon excitation transferred from Ap to the redox counterpart was represented by hole acceptor G. The fluorescence spectroscopy measurements performed for redox-active duplexes were compared with measurements for redox-inactive duplexes in which the hole acceptor G was replaced by redox-inactive inosine (I).

Oligonucleotides were synthesized using the standard phosphoramidite protocol. Synthesis was performed on a 1 μmol scale on [5-*O*-dimethoxytrityl-1-(6-*N*-benzoyladenin-9-yl)-β-D-ribofuranos-3-*O*-succinyl]LCAA-CPG using the Gen-Syn V02 DNA/RNA synthesizer. 2-Aminopurine (Ap) and inosine (I) units were incorporated using commercial phosphoramidites purchased from Glen Research (for details of sample characterization and analysis, and purity and MALDI-MS of prepared oligonucleotides, see Supporting Information).

After the solid-phase synthesis, the column was inserted into the pressure vessel and treated with gaseous ammonia (0.7 MPa) for 16 h to remove acyl protecting groups and to release the product from the solid support. At the end, deprotected DNA was washed out from the column by 0.1 M TEAA buffer and purified by preparative ion exchange chromatography (DNAPac, Dionex).

The UV−vis spectroscopy measurements were performed on a CARY 100 Bio UV Spectrophotometer (Varian Inc.) equipped with a Peltier temperature controller and thermal analysis software. The samples were prepared by mixing together complementary strands in 50 mM sodium phosphate buffer (pH 7.2) to afford 5 μM final concentration. A temperature gradient of 1 °C/min was applied. Melting temperatures (T_m) were determined from the maximum of

dx.doi.org/10.1021/jp501986a | J. Phys. Chem. B XXXX, XXX, XXX−XXX

the first derivative of the absorbance/temperature plots ($T_m \pm 0.5$ °C).

For fluorescence and UV−vis measurements, the synthesized oligomers were dissolved in 50 mM sodium phosphate buffer (pH 7.2); the final duplex concentration was 5 μM. UV−vis spectroscopy was performed with a Varian Carry 50 instrument. As Ap made a band in the 300−340 nm range in absorption spectra, it was possible to selectively excite the Ap. On the basis of comparable Ap absorbance for all the measured samples (0.023 ± 0.001) at 320 nm, the same oligonucleotide concentration was confirmed.

2.2. Fluorescence Spectroscopy. Charge transport was derived from fluorescence quenching measured at the temperatures varying from 5 to 40 °C using steady-state fluorescence spectroscopy (Fluorolog Horiba JY, excitation wavelength 320 nm). To distinguish the fluorescence quenching caused by charge transfer from the fluorescence quenching arising from different processes, the spectroscopic measurements were calibrated against redox-inactive duplexes, where G was replaced by inosine[1,2] (Table 1). Samples with Hg(II) were prepared by using DNA duplexes containing T-T mismatched base pairs; 2 mL of duplexes was blended together with 2 μL (2 equiv) of $HgCl_2$. DNA T-T mismatched samples with added Hg were then heated to 80 °C for 5 min, and after cooling down, the Hg-modified samples were ready for the measurements. Although phosphate buffer may also precipitate with Hg^{2+} along with Hg^{2+} binding to the T-T mismatch, the increase in T_m value measured upon Hg^{2+}-addition to the DNA duplex with a T-T mismatch indicated Hg^{2+}-binding to the T-T mismatch. Accordingly, the difference in fluorescence measured for redox-active and redox-inactive duplexes could be attributed to Hg^{2+}-binding to the T-T mismatch.

2.3. Computational Details. The structural models were DNA duplexes consisting of four base pairs that corresponded to donor G-C and acceptor Ap-T base pairs bridged with two base pairs in the measured oligomers (Table 1 and Figure S1, Supporting Information). The model structures were derived from the original DNA structure with PDB ID 2G1Z[32] having the sequence d(A-A-A-T-T-T)·d(T-T-T-A-A-A). The negative charge of backbone phosphate groups was compensated with six Na^+ ions, the original nucleobases were modified according to the sequences in Table 1, and the hydrogen atoms were added to the PDB structures (Figure 2). The geometry optimizations were carried out employing structural constraints; the initial geometries of all backbone atoms were fixed to preserve the B-DNA structure in the crystal. The B-DNA structural class was recently determined for oligonucleotide containing T-Hg-T base pairs both in the liquid[21] and in the crystal.[23] For the DNA model including the T-T mismatch, we considered their two wobble base pair conformations.[33] The DNA structures including the T-Hg-T base pair were prepared by replacing the two imino hydrogen atoms in T-T mismatch with a mercury atom. In total, four DNA structures were prepared and their geometry optimized. Geometry optimizations of model DNA duplexes were carried out with the Turbomole-6.3.1 quantum chemistry program package,[34] using the B97D[35] energy functional with Grimme's D3[36] dispersion correction, the def2-SVP[37,38] basis set, the RI-J approximation[39] employing auxiliary basis sets,[40] and implicit solvation by water based on COSMO (the conductor-like screening model).[41]

The formation of the T-Hg(II)-T base pair is driven by both enthalpy and entropy.[42] The role of positive reaction entropy was explained only recently.[21,22] The theoretical model of the reaction pathway describing the formation of the T-Hg(II)-T unveiled several states that could be populated in a dynamical regime,[22] especially when the temperature increases. Unfortunately, these states can be hardly captured employing current classical MD procedures, and such a MD simulation would therefore improperly describe the behavior of Hg-DNA. However, the effect of dynamical averaging on the magnitude of calculated coupling integrals in normal nucleic acids may be significant.[43−45] We therefore decided to model the charge transfer efficiency in Hg-DNA oligonucleotide only for the low temperature experiment by employing a B-DNA structural model that was justified experimentally.

The intrastrand charge transfer from donor Ap to acceptor G was assumed, and charge transfer rates were therefore calculated employing nucleobases of the single DNA strand in redox-active DNA duplexes including Ap and G (Figure S1 (Supporting Information) and Table 1); the Ap-A-A-G strand in normal DNA; and the Ap-T-A-G strand in DNA including T-T or the T-Hg-T base pair. For DNA containing the T-T

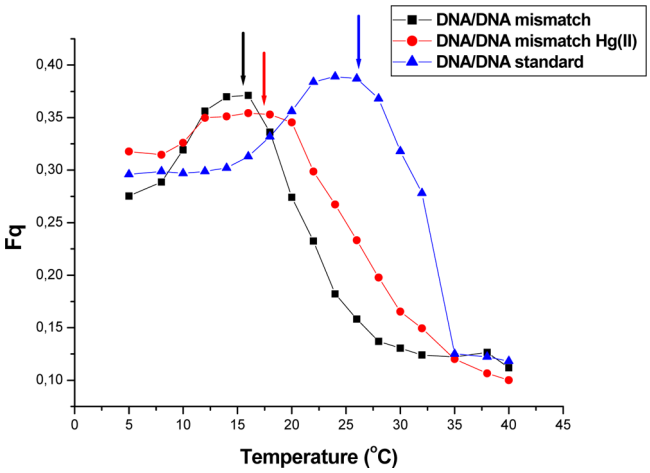

Figure 1. Temperature dependence of quenching efficiency (F_q) for DNA T-T, DNA T-Hg(II)-T, and standard DNA. The arrows above the curves show the duplex melting temperature T_m obtained from UV melting experiments.

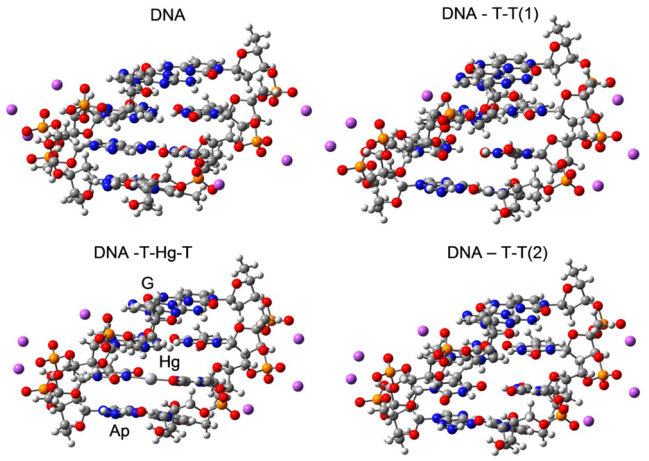

Figure 2. Geometry-optimized structures of model DNA duplexes; normal DNA (DNA), DNA including T-Hg(II)-T (DNA-T-Hg(II)-T), and two alternatives of DNA including T-T (DNA-T-T(1) and DNA-T-T(2)). The position of G and Ap nucleosides in the redox-active strand of the DNA molecule is depicted only for DNA-T-Hg-T. The Na^+ atoms coordinated to phosphate groups are colored violet.

dx.doi.org/10.1021/jp501986a | J. Phys. Chem. B XXXX, XXX, XXX−XXX

mismatch, the two wobble base pair conformations depicted in Figure 3 were calculated. The structural models employed in

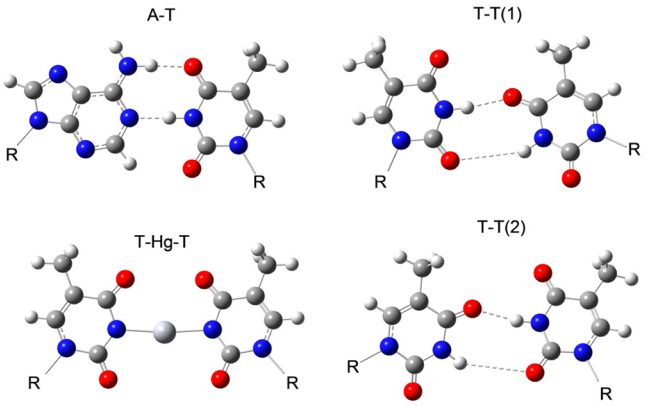

Figure 3. Four alternative base pairs appearing in the same position of model DNA duplexes: A-T base pair in normal DNA, T-Hg-T base pair in Hg-DNA, and two alternative T-T base pairs in DNA containing the T-T mismatch. R stands for the deoxyribose unit in DNA duplexes.

charge transport calculations included only nucleobases extracted from the geometry-optimized DNA duplexes. Their local geometries and mutual positioning were fixed as optimized in the respective DNA duplexes, the sugar-phospate backbone was deleted, and the glycosidic nitrogens were terminated by a hydrogen atom, the position of which was geometry optimized with the DFT-B97D/COSMO/def2-SVP method, keeping all other atoms fixed.

The charge transfer integrals J_{ij}, site energies ε_i, and spatial orbital overlap S_{ij} for two adjacent bases were calculated with the tight-binding method by employing the fragment approach.[46−48] We supposed that the charge transfer mechanism between Ap and G through the adenine bridge was tunnelling (the superexchange approach), as was proposed by Giese.[9] The electronic coupling for the superexchange model was calculated using the effective charge-transfer integral.[48]

$$J_{ij}^{\mathrm{eff}} = J_{ij} - \frac{S_{ij}(\varepsilon_i + \varepsilon_j)}{2} \quad (1)$$

The DFT functional B3LYP,[49] relativistic ZORA (zero order regular approximation),[50−52] the TZ2P[53] Slater type basis set, and the COSMO water model were employed for calculations of charge transfer integrals with the ADF 2012a program package.[54,55] The calculations of electronic coupling $J_{AP,G}$ employed the three dimers consisting of two neighboring pairs of stacked bases as they appear in the DNA strand. The $J_{AP,G}$ electronic coupling (donor−acceptor integral for the superexchange model) was calculated as follows:[60]

$$J_{Ap,G} = \frac{J_{Apb}^{\mathrm{eff}} J_{b'b''}^{\mathrm{eff}} J_{b''G}^{\mathrm{eff}}}{(E_t - E_1)(E_t - E_2)} \quad (2)$$

where effective charge transfer integral $J_{Apb'}^{\mathrm{eff}}$ is computed between donor base Ap and bridging base adjacent to donor b′, $J_{b'b''}^{\mathrm{eff}}$ is computed between two bases of bridge b′ and b″, and $J_{b''G}^{\mathrm{eff}}$ is computed between bridging base adjacent to acceptor b″ and acceptor base G.

E_t is the average value of HOMO and HOMO-1 orbital energies, and E_1 and E_2 correspond to the HOMO-2 and HOMO-3 orbital energies of the tetramer model system, which consisted of three dimers. The charge transfer efficiencies of the individual DNA models were compared on the basis of absolute values of calculated charge transport integrals $|J_{AP,G}|$.

3. RESULTS AND DISCUSSION

3.2. Fluorescence and UV−Vis Spectroscopy. Fluorescence spectroscopy was used to probe charge transfer efficiency in DNA duplexes. The fluorescence was measured at a temperature range from 5 to 40 °C in a series of samples containing redox-inactive and redox-active duplexes (Figure S2a, Supporting Information). The temperature dependence of the fluorescence intensity of redox-active molecules and their redox-inactive analogues were close to each other. The temperature-induced increase of fluorescence was accompanied by a gradual decrease of the excitation band in the 260−290 nm region (Figure S2b, Supporting Information). Since this band is connected to singlet−singlet excitation energy transfer from adjacent bases, its intensity was used for diagnostics of the stacking interactions of Ap.[56,57] The observed effects indicated that temperature caused a weakening of mutual base interactions.

Integrals of fluorescence emission spectra over wavelengths were expressed (at each relevant temperature point) for redox-active (Φ_G) and redox-inactive duplexes (Φ_I). Importantly, the redox-active duplexes' fluorescence was always lower compared to that of the redox-inactive duplexes. This decrease was attributed to the quenching caused by charge transfer.[39] The quenching efficiencies were calculated as $F_q = 1-\Phi_G/\Phi_I$ (Figure 1 and Table S1, Supporting Information). The higher F_q value corresponds to higher charge transfer through the part of the DNA chain between Ap and G.

The highest overall quenching at 5 °C was obtained for the T-Hg(II)-T DNA; this complex has the best charge transfer properties at temperatures when the duplexes are fully hybridized into a double strand, and the base dynamics is rather limited. DNA with the T-T mismatch but without Hg(II) had lower quenching at 5 °C than standard DNA duplexes.

As the temperature increased, the fluorescence quenching efficiencies F_q of all samples were rising (Figure 1); even this effect can be attributed to the weakening of the interactions of the bases and higher probability that bases adopted suitable positions for charge transfer more frequently.

At one temperature point (specific for each sample) F_q dropped down with the highest probability due to conformational changes during dissociation of the duplex. For standard DNA, the charge transfer yield increased with temperature up to 26 °C and after this temperature decreased continually. For DNA T-T, the charge transfer yield increased up to 17 °C, and the increase of charge transfer efficiency of DNA T-Hg(II)-T was observed up to 20 °C. Thus, in the case of the DNA mismatched duplex, the charge transfer yield break point increased significantly (+3 °C) after adding Hg to the solution due to the fact that T-Hg(II)-T improved the DNA mismatched system resistivity against the temperature dissociation.

The maximal charge transfer efficiency (F_q value) was observed for standard DNA and the lowest efficiency was observed for DNA T-Hg (II)-T. The lower charge transfer efficiency for T-T mismatched duplexes compared to that of

dx.doi.org/10.1021/jp501986a | J. Phys. Chem. B XXXX, XXX, XXX−XXX

standard DNA is in accordance with the generally accepted picture, where the perturbed π stacking is crucially important in the charge transfer processes through DNA.[14,58−62]

The temperature dependence of UV−vis and fluorescence correlated well between both analytical methods. The UV−vis spectroscopy showed that for the DNA mismatched duplex, the melting point increased (+2 °C) by adding Hg to the solution: the T-Hg(II)-T complex stabilized the system and made it more resistant against melting (Figure S3, Supporting Information).

3.3. Computer Modeling. In order to evaluate the effect of mercury on charge transfer efficiency, we compared the donor−acceptor charge transfer integrals $|J_{AP,G}|$ calculated for normal DNA duplexes with those for DNA duplexes containing a T-T mismatch or a T-Hg-T base pair (Table 2). The $|J_{AP,G}|$ for normal DNA was smaller than $|J_{AP,G}|$ for DNA including T-Hg-T and larger than $|J_{AP,G}|$ for DNA including the T-T mismatch. The calculated donor−acceptor couplings thus agreed with the charge transfer measurements at low temperature (Figure 1).

Table 2. Effective Charge Transfer Integrals for Pairs of Adjacent Bases and the Donor−Acceptor Couplings $|J_{AP,G}|$ in meV Calculated for the Redox-Active DNA Duplexes

duplex	sequence	$J^{eff}_{Apb'}$	$J^{eff}_{b'b''}$	$J^{eff}_{b''G''}$	$\|J_{Ap,G}\|$
normal DNA	Ap-A-A-G	205.1	29.3	37.7	4.1
DNA including T-T	Ap-T_1-A-G[a]	−156.9	−90.0	1.2	0.2
DNA including T-T	Ap-T_2-A-G[a]	−18.8	−77.0	−60.1	1.4
DNA including T-Hg-T	Ap-T(HgT)-A-G[b]	−110.5	−82.7	33.2	5.5
DNA including T-Hg-T	Ap-T-A-G[c]	−109.2	−81.0	33.2	4.7
DNA including T-Hg-T	Ap-T(T)-A-G[d]	−103.2	−85.7	33.2	4.5

[a]The two alternative mismatched T-T base pairs depicted in Figure 3 were employed. [b]The complete T-Hg-T base pair was employed in the charge transfer efficiency calculation. [c]Only the T base of the redox-active strand was employed in the charge transfer efficiency calculation. [d]The mercury atom was removed, i.e., the T-T mismatched base pair with the local geometry of T bases as was optimized for T-Hg-T base pair was employed in the charge transfer efficiency calculation.

The effect of the T-Hg(II)-T base pair on the calculated charge transport through the redox-active DNA strand was relatively large. The respective $|J_{AP,G}|$ was 5.5 meV, while that for DNA including the mismatched T-T base pair was only 0.2 or 1.4 meV depending on the local geometry of T-T shown in Figure 3. An important question is whether the calculated effect on the charge transport efficiency comes from different geometries or whether it comes from a different electronic structure of the T base in T-T and T-Hg-T base pairs. To answer this question, we calculated the $|J_{AP,G}|$ coupling integrals employing the same model structure but including the complete T-Hg-T base pair. When the effect of mercury bonding on the electronic state of the T base was included (calculation c in Table 2), $|J_{AP,G}|$ was 5.5 meV. When the mercury atom was removed from the base pair (calculation d in Table 2), $|J_{AP,G}|$ was 4.7 meV. The larger donor−acceptor coupling for DNA containing T-Hg-T compared to that of DNA containing T-T mismatch was therefore more likely obtained owing to local geometry than owing to a different electronic state of the T base in the T-T or T-Hg-T base pair. The calculated charge transfer integrals for pairs of adjacent bases indicated that mutual positioning of stacked bases close to Ap is essential for the magnitude of donor−acceptor couplings (Table 2). In this respect, the mercury atom linking T bases in the T-Hg-T base pair is known to ensure the geometry of a metal-mediated base pair that is very similar to standard DNA base pairs.[21,23] The donor−acceptor couplings for standard DNA and DNA including T-Hg-T were therefore larger than the couplings for DNA including the T-T mismatched base pair. We may also assume that the T-T mismatch should be more structurally disordered compared to that of standard DNA or DNA including T-Hg-T when considering the temperature increase that results in large amplitude motions of the nucleobases. The mercury linkage in T-Hg-T was recently characterized as covalent.[24,25] The assumption of structurally disordered T-T may explain the decrease of charge transport efficiency of T-T mismatched DNA compared to that of charge transport efficiencies of standard DNA and DNA including T-Hg-T (Figure 1).

Charge transfer in oligonucleotides is a very complex phenomenon, and many parameters may play specific roles.[1,2,9,14] In our case, it is namely the spatial overlap of bases that substantially influenced the calculated charge transfer rates, and the overlap of bases was markedly affected by the presence of Hg(II) linkage in the T-T mismatch. Our calculations show that Hg orbitals do not contribute to the HOMO and HOMO-1 orbitals (this conclusion corresponds with results of Voityuk),[61] and therefore, Hg orbitals cannot directly influence the charge transport properties. The chemical reaction for the formation of the T-Hg-T base pair proposed and calculated in agreement with available experimental data suggests that the Hg atom may be exchangeable with two bulk protons.[22] With the temperature increase, we may thus assume that both T-T and T-Hg-T base pairs will be populated. The structural distortion of a normal DNA duplex that can be expected with the temperature increase is thus consistent with the measured decrease of charge transport efficiency for high temperatures (Figure 1).

4. SUMMARY

The main goal of this article was to investigate the impact of mercury bonded on DNA mismatched bases on the charge transfer process. For this purpose, we measured the temperature dependence of steady-state fluorescence of standard DNA, DNA with a mismatched (T-T) base pair, and DNA containing T-Hg-T. Experimental results were confronted with a theoretical approach: density functional theory.

At low temperatures, the highest overall quenching of fluorescence (and therefore the highest rate of charge transfer) was obtained for the DNA mismatch with Hg(II). Mismatched DNA without Hg(II) had lower quenching than standard DNA duplexes.

For all the systems under study, the charge transfer yield increased with temperature up to a breaking point that was specific for each type of sample. Fluorescence spectroscopy measurements (fluorescence quenching and excitation band intensity) indicated that temperature caused the weakening of mutual base interactions and thus activated the charge transfer. For temperatures above the breaking point, the charge transfer rapidly decreased. Temperature at the breaking point of the mismatched DNA duplex increased after adding Hg to the solution. These results were in good correlation with UV−vis spectroscopy measurements: the lowest melting point was manifested by DNA T-T duplexes and the highest by standard DNA samples.

dx.doi.org/10.1021/jp501986a | J. Phys. Chem. B XXXX, XXX, XXX−XXX

Our experimental results were confronted with quantum chemistry models. Calculations indicated that the changes in charge transfer were likely owing to the differences in local geometry (overlap of bases) than due to the electronic structure. Models showed that Hg orbitals did not contribute to HOMO and HOMO-1, and therefore Hg orbitals could not directly influence the charge transport properties.

Our theoretical and experimantal study allowed us to make a model of our sample states and behavior as follows: At low temperatures, the charge transfer conditions were poorest for the most structurally disordered DNA T-T. On the contrary, for DNA T-Hg(II)-T, the bases between donor and acceptor were at low temperatures in such positions that the overlap of the bases was most favorable for charge transfer. Rising temperature generally improved charge transfer in all cases, and due to the sufficient thermal motions, the bases adopted suitable positions more frequently. For standard DNA, the temperature-enhanced dynamics enabled such an overlap of bases that charge transfer closely under break point was the best from all of the systems under study. However, with increasing temperature, Hg bound to the T-Hg(II)-T system eventually limited the thermal motion by which the charge transfer was otherwise facilitated, thereby reducing the charge transfer. In all cases, as a consequence of conformational changes connected with duplexes melting the charge transfer efficiency declined at temperatures above break points. T-Hg(II)-T formation stabilized the whole system and improved the resistance of the mismatched DNA to melting.

We present the link between the efficiency of charge transfer and basic physicochemical properties of metal−oligonucleotide complexes. DNA/Hg complexes play an important role in the sensing of defects in DNA or the presence of Hg in the environment. Our investigation of a metallo-DNA duplex provides the basis for the design of metal-conjugated nucleic acid nanomaterials.

■ ASSOCIATED CONTENT

Ⓢ Supporting Information

Chemical structure of the DNA redox-active duplex; temperature dependence of quenching efficiency for T-T mismatched DNA, DNA T-T mismatched Hg(II) containing duplexes, and standard DNA; temperature dependence and emission/excitation spectra of DNA mismatch redox active samples; and thermal characteristics/melting temperatures of active DNA, active DNA with T-T mismatch, and active DNA with T-T mismatch and Hg(II) added. This material is available free of charge via the Internet at http://pubs.acs.org.

■ AUTHOR INFORMATION

Corresponding Authors

*(I.K.) Tel: +420 266 052 524. Fax: +420 286 890 527. E-mail: krat@fzu.cz.

*(O.P.) Tel:+420 220 183 244. Fax: +420 220 183 531. E-mail: pav@uochb.cas.cz.

Notes

The authors declare no competing financial interest.

■ ACKNOWLEDGMENTS

We gratefully acknowledge the support by grants TA01011165, 14-10279S, 13-29358S, 13-26526S, and 15-21387S. Computer time at the MetaCentrum and the support by the IOCB research project RVO:61388963 are also gratefully acknowledged.

■ REFERENCES

(1) Wagenknecht, H. A. *Charge Transfer Process in DNA: From Mechanism to Application*; Wiley-Vch Verlag Gmbh & Co. KGaA: Weinheim, Germany, 2005.

(2) Genereux, J. C.; Wuerth, S. M.; Barton, J. K. Single-Step Charge Transport through DNA over Long Distances. *J. Am. Chem. Soc.* **2011**, *133*, 3863−3868.

(3) Matsui, T.; Shigeta, Y.; Hirao, K. Multiple Proton-Transfer Reactions in DNA Base Pairs by Coordination of Pt Complex. *J. Phys. Chem. B* **2007**, *111*, 1176−1181.

(4) Tang, Y. L.; He, F.; Yu, M. H.; Feng, F. D.; An, L. L.; Sun, H.; Wang, S.; Li, Y. L.; Zhu, D. B. A Reversible and Highly Selective Fluorescent Sensor for Mercury(II) Using Poly (thiophene)s That Contain Thymine Moieties. *Macromol. Rapid Commun.* **2006**, *27*, 389−392.

(5) Wang, Z.; Zhang, D. Q.; Zhu, D. B. A Sensitive and Selective "Turn On" Fluorescent Chemosensor for Hg(II) Ion Based on a New Pyrene-Thymine Dyad. *Anal. Chim. Acta* **2005**, *549*, 10−13.

(6) Kratochvílová, I.; Král, K.; Bunček, M.; Víšková, A.; Nešpůrek, S.; Kochalska, A.; Todorciuc, T.; Weiter, M.; Schneider, B. Conductivity of Natural and Modified DNA Measured by Scanning Tunneling Microscopy. The Effect of Sequence, Charge and Stacking. *Biophys. Chem.* **2008**, *138*, 3−10.

(7) Kratochvílová, I.; Todorciuc, T.; Král, K.; Němec, H.; Bunček, M.; Šebera, J.; Záliš, S.; Vokáčová, Z.; Sychrovský, V.; Bednárová, L.; et al. Charge Transport in DNA Oligonucleotides with Various Base-Pairing Patterns. *J. Phys. Chem. B* **2010**, *114*, 5196−5205.

(8) Kratochvílová, I.; Vala, M.; Weiter, M.; Špérová, M.; Schneider, B.; Páv, O.; Šebera, J.; Rosenberg, I.; Sychrovský, V. Charge Transfer through DNA/DNA Duplexes and DNA/RNA Hybrids: Complex Theoretical and Experimental Studies. *Biophys. Chem.* **2013**, *180*, 127−134.

(9) Giese, B. Long-Distance Electron Transfer through DNA. *Annu. Rev. Biochem.* **2002**, *71*, 51−70.

(10) Wohlgamuth, C. H.; McWilliams, M. A.; Slinker, J. D. Temperature Dependence of Electrochemical DNA Charge Transport: Influence of a Mismatch. *Anal. Chem.* **2013**, *85*, 1462−1467.

(11) O'Neill, M. A.; Barton, J. K. 2-aminopurine: A Probe of Structural Dynamics and Charge Transfer in DNA and DNA: RNA Hybrids. *J. Am. Chem. Soc.* **2002**, *124*, 13053−13066.

(12) Kratochvílová, I.; Kovalenko, A.; Fendrych, F.; Petráková, V.; Záliš, S.; Nesládek, M. Tuning of Nanodiamond Particles' Optical Properties by Structural Defects and Surface Modifications: DFT Modelling. *J. Mater. Chem.* **2011**, *21*, 18248.

(13) Kratochvílová, I.; Král, K.; Bunček, M.; Nešpůrek, S.; Todorciuc, T.; Weiter, M.; Navrátil, J.; Schneider, B.; Pavluch, J. Scanning Tunneling Spectrosopy Study of DNA Conductivity. *Cent. Eur. J. Phys.* **2008**, *6*, 422−426.

(14) Kawai, K.; Majima, T. Hole Transfer Kinetics of DNA. *Acc. Chem. Res.* **2013**, *46*, 2616−2625.

(15) Pan, Z.; Hariharan, M.; Arkin, J. D.; Jalilov, A. S.; McCullagh, M.; Schatz, G. C.; Lewis, F. D. Electron Donor-Acceptor Interactions with Flanking Purines Influence the Efficiency of Thymine Photodimerization. *J. Am. Chem. Soc.* **2011**, *133*, 20793−20798.

(16) Pan, Z.; McCullagh, M.; Schatz, G. C.; Lewis, F. D. Conformational Control of Thymine Photodimerization in Purine-Containing Trinucleotides. *J. Phys. Chem. Lett.* **2011**, *2*, 1432−1438.

(17) Mašek, J.; Bartheldyová, E.; Turánek-Knotigová, P.; Škrabalová, M.; Korvasová, Z.; Plocková, J.; Koudelka, Š.; Škodová, P.; Kulicha, P.; Křupka, M.; et al. Metallochelating Liposomes with Associated Lipophilised norAbuMDP as Biocompatible Platform for Construction of Vaccines with Recombinant His-Tagged Antigens: Preparation, Structural Study and Immune Response towards rHsp90. *J. Controlled Release* **2011**, *151*, 193−201.

(18) Kratochvilova-Hruba, I.; Gregora, I.; Pokorny, J.; Kamba, S.; Zikmund, Z.; Petzelt, J.; Cernansky, M.; Studnicka, V.; Sigaev, V. N.;

Smelyanskaya, E. N. Vibrational Spectroscopy of LaBSiO5 Glass and Glass-Crystal Composites. *J. Non-Cryst. Solids* **2001**, *290*, 224−230.
(19) Wohlgamuth, C. H.; McWilliams, M. A.; Slinker, J. D. DNA as a Molecular Wire: Distance and Sequence Dependence. *Anal. Chem.* **2013**, *85*, 8634−8640.
(20) Tanaka, Y.; Oda, S.; Yamaguchi, H.; Kondo, Y.; Kojima, C.; Ono, A. ^{15}N-^{15}N J-Coupling across Hg^{II}: Direct Observation of Hg^{II}-Mediated T-T Base Pairs in a DNA Duplex. *J. Am. Chem. Soc.* **2007**, *129*, 244−245.
(21) Yamaguchi, H.; Šebera, J.; Kondo, J.; Oda, S.; Komuro, T.; Kawamura, T.; Dairaku, T.; Kondo, Y.; Okamoto, I.; Ono, A. The Structure of Metallo-DNA with Consecutive Thymine−Hg^{II}−Thymine Base Pairs Explains Positive Entropy for the Metallo Base Pair Formation. *Nucleic Acids Res.* **2014**, *42*, 4094−4099.
(22) Šebera, J.; Burda, J.; Straka, M.; Ono, A.; Kojima, C.; Tanaka, Y.; Sychrovský, V. Formation of a Thymine-Hg^{II}-Thymine Metal-Mediated DNA Base Pair: Proposal and Theoretical Calculation of the Reaction Pathway. *Chem.—Eur. J.* **2013**, *19*, 9884−9894.
(23) Kondo, J.; Yamada, T.; Hirose, C.; Okamoto, I.; Tanaka, Y.; Ono, A. Crystal Structure of Metallo DNA Duplex Containing Consecutive Watson−Crick-Like T−Hg^{II}−T Base Pairs. *Angew. Chem., Int. Ed.* **2014**, *53*, 2385−2388.
(24) Uchiyama, T.; Miura, T.; Takeuchi, H.; Dairaku, T.; Komuro, T.; Kawamura, T.; Kondo, Y.; Benda, L.; Sychrovský, V.; Bouř, P.; et al. Raman Spectroscopic Detection of the T-Hg(II)-T Base Pair and the Ionic Characteristics of Mercury. *Nucleic Acids Res.* **2012**, *40*, 5766−5774.
(25) Miyake, Y.; Togashi, H.; Tashiro, M.; Yamaguchi, H.; Oda, S.; Kudo, M.; Tanaka, Y.; Kondo, Y.; Sawa, R.; Fujimoto, T.; et al. $Mercury^{II}$-Mediated Formation of Thymine-Hg^{II}-Thymine Base Pairs in DNA Duplexes. *J. Am. Chem. Soc.* **2006**, *128*, 2172−2173.
(26) Hiroyuki, I.; Yamazaki, N.; Atsushi, A.; Fujino, T.; Nakanishi, W.; Seki, S. Electron Mobility in a Mercury-Mediated Duplex of Triazole-Linked DNA (TLDNA). *Chem. Lett.* **2011**, *40*, 318−319.
(27) Guo, L.; Hu, H.; Sun, R.; Chen, G. Highly Sensitive Fluorescent Sensor for Mercury Ion Based on Photoinduced Charge Transfer between Fluorophore and π-Stacked T−Hg(II)−T Base Pairs. *Talanta* **2009**, *79*, 775−779.
(28) Guo, L.; Yin, N.; Chen, G. Photoinduced Electron Transfer Mediated by π-Stacked Thymine-Hg^{2+}-Thymine Base Pairs. *J. Phys. Chem. C* **2011**, *115*, 4837−4842.
(29) Ito, T.; Nikaido, G.; Nishimoto, S. Effects of Metal Binding to Mismatched Base Pairs on DNA-Mediated Charge Transfer. *J. Inorg. Biochem.* **2007**, *101*, 1090−1093.
(30) Joseph, J.; Schuster, G. B. Long-Distance Radical Cation Hopping in DNA: The Effect of Thymine-Hg(II)-Thymine Base Pairs. *Org. Lett.* **2007**, *9*, 1843−1846.
(31) Miyachi, H.; Matsui, T.; Shigeta, Y.; Hirao, K. Effects of Mercury(II) on Structural Properties, Electronic Structure and UV Absorption Spectra of a Duplex Containing Thymine-Mercury(II)-Thymine Nucleobase Pairs. *Phys. Chem. Chem. Phys.* **2010**, *12*, 909−917.
(32) Valls, N.; Santaolalla, A.; Campos, J. L.; Subirana, J. A. Packing Features of the All-AT Oligonucleotide d(AAATTT). *J. Biomol. Struct. Dyn.* **2007**, *34*, 24547−53.
(33) Trotta, E.; Paci, M. Solution Structure of DAPI Selectively Bound in the Minor Groove of a DNA T.T Mismatch-Containing Site: NMR and Molecular Dynamics Studies. *Nucleic Acids Res.* **1998**, *26*, 4706−4713.
(34) Ahlrichs, R.; Bar, M.; Haser, M.; Horn, H.; Kolmel, C. Electronic Structure Calculations on Workstation Computers: The Program System Turbomole. *Chem. Phys. Lett.* **1989**, *162*, 165−169.
(35) Grimme, S. Semiempirical GGA-Type Density Functional Constructed with a Long-Range Dispersion Correction. *J. Comput. Chem.* **2006**, *27*, 1787−1789.
(36) Grimme, S.; Antony, J.; Ehrlich, S.; Krieg, H. A Consistent and Accurate ab initio Parametrization of Density Functional Dispersion Correction (DFT-D) for the 94 Elements H-Pu. *J. Chem. Phys.* **2010**, *132*, 154104−154119.
(37) Weigend, F.; Ahlrichs, R. Balanced Basis Sets of Split Valence, Triple Zeta Valence and Quadruple Zeta Valence Quality for H to Rn: Design and Assessment of Accuracy. *Phys. Chem. Chem. Phys.* **2005**, *7*, 3297−3305.
(38) Schäfer, A.; Horn, H.; Ahlrichs, R. Fully Optimized Contracted Gaussian-Basis Sets for Atoms Li to Kr. *J. Chem. Phys.* **1992**, *97*, 2571−2577.
(39) Furche, F.; Rappoport. D. In *Computational Photochemistry*; Olivucci, M., Ed.; Band 16 von Computational and Theoretical Chemistry, Kapitel III; Elsevier: Amsterdam, 2005.
(40) Weigend, F. Accurate Coulomb-Fitting Basis Sets for H to Rn. *Phys. Chem. Chem. Phys.* **2006**, *8*, 1057−1065.
(41) Klamt, A.; Schüürmann, G. Cosmo - A New Approach to Dielectric Screening in Solvents with Explicit Expressions for the Screening Energy and Its Gradient. *J. Chem. Soc., Perkin Trans.* **1993**, *2*, 799−805.
(42) Torigoe, H.; Ono, A.; Kozasa, T. Hg^{II} Ion Specifically Binds with T:T Mismatched Base Pair in Duplex DNA. *Chem.—Eur. J.* **2010**, *16*, 13218−13225.
(43) Troisi, A.; Orlandi, G. Hole Migration in DNA: A Theoretical Analysis of the Role of Structural Fluctuations. *J. Phys. Chem. B* **2002**, *106*, 2093−2101.
(44) Řeha, D.; Barford, W.; Harris, S. A Multi-Scale Method for the Calculation of Charge Transfer Rates through the Pi-Stack of DNA: Application to DNA Dynamics. *Phys. Chem. Chem. Phys.* **2008**, *10*, 5436−5444.
(45) Kubař, T.; Gutierrez, R.; Kleinekathofer, U.; Cuniberti, G.; Elstner, M. Modeling Charge Transport in DNA Using Multi-Scale Methods. *Phys. Status Solidi B* **2013**, *250*, 2277−2287.
(46) Newton, M. D. Quantum Chemical Probes of Electron-Transfer Kinetics: the Nature of Donor-Acceptor Interactions. *Chem. Rev.* **1991**, *91*, 767−792.
(47) Senthilkumar, K.; Grozema, F. C.; Bickelhaupt, F. M.; Siebbeles, L. D. A. Charge Transport in Columnar Stacked Triphenylenes: Effects of Conformational Fluctuations on Charge Transfer Integrals and Site Energies. *J. Chem. Phys.* **2003**, *119*, 9809−9817.
(48) Senthilkumar, K.; Grozema, F. C.; Fonseca Guerra, C.; Bickelhaupt, F. M.; Lewis, F. D.; Berlin, Y. A.; Ratner, M. A.; Siebbeles, L. D. A. Absolute Rates of Hole Transfer in DNA. *J. Am. Chem. Soc.* **2005**, *127*, 14894−14903.
(49) Becke, A. D. Density - Functional Thermochemistry. III. The Role of Exact Exchange. *J. Chem. Phys.* **1993**, *98*, 5648−5652.
(50) van Lenthe, E.; Ehlers, A. E.; Baerends, E. J. Geometry Optimization in the Zero Order Regular Approximation for Relativistic Effects. *J. Chem. Phys.* **1993**, *110*, 8943−8953.
(51) van Lenthe, E.; Baerends, E. J.; Snijders, J. G. Relativistic Regular 2-Component Hamiltonians. *J. Chem. Phys.* **1993**, *99*, 4597−4610.
(52) van Lenthe, E.; Baerends, E. J.; Snijders, J. G. Relativistic Total Energy Using Regular Approximations. *J. Chem. Phys.* **1994**, *101*, 9783−9792.
(53) van Lenthe, E.; Baerends, E. J. Optimized Slater-Type Basis Sets for the Elements 1−118. *J. Comput. Chem.* **2003**, *24*, 1142−1156.
(54) Fonseca Guerra, C.; Snijders, J. G.; teVelde, G.; Baerends, E. J. Towards an Order-N DFT Method. *Theor. Chem. Acc.* **1998**, *99*, 391−403.
(55) teVelde, G.; Bickelhaupt, F. M.; S. van Gisbergen, J. A.; Fonseca Guerra, C.; Baerends, E. J.; Snijders, J. G.; Ziegler, T. Chemistry with ADF. *J. Comput. Chem.* **2001**, *22*, 931−967.
(56) Nordlund, T. M.; Xu, D.; Evans, K. O. Excitation energy transfer in DNA: Duplex melting and transfer from normal bases to 2-aminopurine. *Biochemistry* **1993**, *32*, 12090−12095.
(57) Hochstrasser, R. A.; Carver, T. E.; Sowers, L. C.; Millar, D. P. Melting of a DNA Helix Terminus within the Active Site of a DNA Polymerase. *Biochemistry* **1994**, *33*, 11971−11979.
(58) Takada, T.; Takeda, Y.; Fujitsuka, M.; Majima, T. "Signal-On" Detection of DNA Hole Transfer at the Single Molecule Level. *J. Am. Chem. Soc.* **2009**, *131*, 6656−6657.

672 (59) Osakada, Y.; Kawai, K.; Fujitsuka, M.; Majima, T. Kinetics of
673 charge transfer in DNA containing a mismatch. *Nucleic Acids Res.*
674 **2008**, *36*, 5562−5570.
675 (60) Voityuk, A. A. Electronic Couplings in DNA π-Stacks:
676 Multistate Effects. *J. Phys. Chem. B* **2005**, *109*, 17917−19721.
677 (61) Voityuk, A. A. Electronic Coupling Mediated by Stacked
678 [Thymine-Hg-Thymine] Base Pairs. *J. Phys. Chem. B* **2006**, *110*,
679 21010−21013.
680 (62) O'Neill, M. A.; Barton, J. K. DNA-Mediated Charge Transport
681 Requires Conformational Motion of the DNA Bases: Elimination of
682 Charge Transport in Rigid Glasses at 77 K. *J. Am. Chem. Soc.* **2004**,
683 *126*, 13232−13233.